

Assessment of RELAP5/MOD3.2.2g Against Flooding Database in Horizontal-to-Inclined Pipes

Hyoung Tae Kim and Hee Cheon NO

Korea Advanced Institute of Science and Technology
373-1, Kusong-Dong, Yusong-Gu, Taejon, 305-701, Korea

Abstract

A total of 356 experimental data for the onset of flooding are compiled for the data bank and used for the assessment of RELAP5/MOD3.2.2g predictions of Counter-Current Flow Limitation (CCFL) in horizontal-to-inclined pipes simulating a PWR hot leg.

The predictions of the flooding gas velocity in the database are known to be largely dependent on the horizontal pipe length-to-diameter ratio (L/D). RELAP5 calculations are compared with the experimental data where L/D is varied within the range of database. The present input model used for the simulation of CCFL is validated to reasonably calculate the gradient of water level in the horizontal pipes connected with the inclined volumes.

RELAP5 calculations show that the RELAP5 predicts the flooding points qualitatively well but higher gas flow rate is required to initiate the flooding compared with the experimental data if the L/D is as low as that of the hot legs of typical PWRs.

Standard RELAP5 code is modified to apply the user specified CCFL curve not only to vertical volumes but also to the horizontal volumes. The calculation value by the modified version lies well on the applied CCFL curve even if flooding occurs at lower gas velocity than predicted by the CCFL curve in standard RELAP5.

1. Introduction

Counter-current flow of steam and water can be observed in the hot leg during emergency core cooling following a Loss-of Coolant Accident (LOCA). When saturated water condensed in the Steam Generator (SG) tubes drains back down into the reactor vessel via the hot leg (reflux condensation cooling mode), the possibility that steam previously boiled off in the core could partly or totally inhibit the water back down flow is one of the important concerns regarding the safety analysis of the Pressurized Water Reactor (PWR).

A general CCFL model [3] was implemented in RELAP5/MOD3 that allows the user to select the Wallis form, the Kutateladze form, or a form in between the Wallis and Kutateladze forms:

$$H_g^{1/2} + m H_f^{1/2} = c, \quad (1)$$

where subscript f is for liquid phase, subscript g is for gas phase, m is a slope and c is a gas intercept and the dimensionless fluxes have the form:

$$H_k = j_k \left[\frac{\mathbf{r}_k}{g w (\mathbf{r}_f - \mathbf{r}_g)} \right]^{1/2}, \quad k = f, g \quad (2)$$

where j_k is the superficial velocity for each phase, g is a gravitational acceleration and w is given by the expression:

$$w = D^{1-b} L^b, \quad (3)$$

where D is a junction hydraulic diameter and L is the Laplace capillary constant given by:

$$L = \left[\frac{\sigma}{g (\mathbf{r}_f - \mathbf{r}_g)} \right]^{1/2}, \quad (4)$$

where σ is the surface tension. In Eq. (3), β can be a number from 0 to 1. For $\beta=0$, the Wallis form of the CCFL equation is obtained, and for $\beta=1$, the Kutateladze form of CCFL equation is obtained. For $0 < \beta < 1$, a combination of the Wallis and Kutateladze form is obtained. The RELAP5 input is made general so that the user can input CCFL correlations for the particular geometry of interest in the volumes with the inclination angle over than 45° .

From the experiments of the flooding in horizontal-to-inclined pipes it is known that the hydraulic jump and the instability of the gas-liquid interface in the horizontal pipe induce the onset of flooding. To use the CCFL curve given by user also in the horizontal volumes NO and Heo [4] extended the CCFL model of RELAP5 for the vertical volumes ($>45^\circ$) to the horizontal volumes and enabled the user to input the information of length-to-diameter ratio (L/D) into the gas intercept, c in Eq. (1). However if the flooding limit by the interfacial and the wall drags are higher than that by the flooding curve, NO's model cannot be applied to the simulation of CCFL in the horizontal volumes. In the present study the interfacial and the wall drags are reduced when flooding occurs at lower gas velocity than predicted by the CCFL curve in standard RELAP5.

Experimental results for flooding in horizontal pipes connected with inclined riser are available for the assessment of RELAP5 code for the flooding in a PWR hot leg. The focus of these experimental studies has been to obtain the fluid velocities at the onset of flooding under various geometries. The most commonly used flooding correlation has been the linear relationship expressed in Wallis-type correlation as shown in Eq. (1)

with $\beta=0$. From 8 references a literature survey compiled a data bank containing 356 dimensionless Wallis-type gas velocities and liquid velocities identified with the geometrical conditions such as horizontal pipe diameter (D), length (L) and the inclination angle (θ) of the bend. Figure 1 shows the general configuration of the CCFL test facility.

From the sample problems to test how RELAP5 code predicts the CCFL behavior in a pipe RELAP5 nodalizations have been developed for the simulation of the experiments in the database. To simulate the experimental results the geometries of the horizontal-to-inclined pipes in RELAP5 model are maintained as same as those of the experimental conditions. The parametric effects on flooding are investigated by comparing RELAP5 results with the experimental data selected from the data bank covering a wide range of the parameters.

2. The Flooding Database

From the literature survey a considerable amount of flooding data has been collected together to form a data bank containing 356 flooding points. Most of data points are the measurements of the onset of flooding limits in air-water counter-current flows in horizontal tubes connected at the water inlet to the elbows with the inclination angles from 35° to 90° . Table 1 summarizes the sources of flooding data and gives details of tube geometries and the inclination angles of bends. Figure 2 presents the flooding data points in graphical form and the dimensionless gas and liquid velocities are the dimensionless superficial velocities from the Wallis form of CCFL equation.

In the experiments by Kawaji [8], Wongwises [10], and Kang [11], the flooding curve was divided into three regions due to a change in the flooding mechanism. In these cases the flooding data points are confined to the first region [10], where the air flow rate that creates the onset of flooding decreases, while the water flow rate increases. Therefore, all the flooding data points obtained are close to the widely accepted Wallis correlation.

The experiments on flooding in horizontal-to-inclined pipes were conducted over different conditions, such as tube diameter (D), length (L), inclination of the elbow (θ), radius of curvature of the elbow and inlet or exit geometry of tube. The data bank is biased towards air-water flow (90 % of the data) and 96% of data is for tubes of diameter less than 80 mm. Most researchers (Ohnuki [5], Siddiqui [7], Wongwises, Kang) found that flooding limit in a horizontal-to-inclined pipe is strongly dependent on the length-to-diameter ratio (L/D) within the range of experimental tests. The effects of other parameters are not clear and inappropriate for RELAP5 code modelling except the parameter, θ .

Therefore, 2 parametric effects, L/D and θ on flooding limits are investigated in this study. And the effects of geometric parameters on CCFL are used to correlate all the data in Table 1 by the linear relationship expressed in Wallis-type correlation.

2.1 Length-to-Diameter Ratio (L/D) Effect on CCFL

Ohnuki, Siddiqui, Wongwises, and Kang performed experiments in which the length of the horizontal pipe was varied. According to their results a longer horizontal length causes the water level to be higher in the vicinity of the bend due to an increase in frictions at the wall and interface and slows down the water flow. This, in turn, induces a higher gas velocity and hence an earlier formation of unstable wave growth at the hydraulic jump.

The CCFL data obtained from the data bank with 4 different L/Ds are shown in Fig. 3. These 4 data sets are selected such that they represent various ranges of L/D from the different sources of experiments as possible. Since a larger L/D corresponds to a longer horizontal pipe length for a given pipe diameter, the lower L/D, the higher the flooding curve in Fig. 3.

2.2 Inclination Angle (θ) of Elbow Effect on CCFL

The variation of the inclination angle (θ) of elbow in the present data bank is from 35° to 90° . To compare the flooding points for different inclination angle of elbow, 3 data sets from Wongwises ($L/D = 22$) and 1 data set from Kang ($L/D = 25$) are selected and plotted in Fig. 4. The flooding points with different θ show the similar results indicating that θ effect is not so clear as in the case of L/D effect on CCFL.

2.3 Development of Empirical Flooding Correlation

Most of the existing data on CCFL are empirically correlated by the Wallis correlations as:

$$j_g^{*0.5} + m j_f^{*0.5} = c \quad (5)$$

Knowing that the deviation of the data points in Fig. 2 is mainly due to the L/D effect, the best fitting correlation is developed for the prediction of flooding points. The regression of the existing data points are conducted to find the constant m for the slope of flooding curve and the gas intercept, c. The results of empirical correlations based on the present data bank are as follows:

$$j_g^{*0.5} + 0.614 j_f^{*0.5} = 0.635 - 0.00254 \left(\frac{L}{D} \right) \quad (6)$$

The L/D effect on CCFL is also considered in the Ohnuki's correlation [5] and Kang's correlation [11].

$$j_g^{*0.5} + 0.75 j_f^{*0.5} = \ln \left[\left(\frac{L}{D} \right) \left(\frac{1}{I} \right) \right]^{-0.066} + 0.88, \quad \text{for Ohnuki's correlation} \quad (7)$$

$$j_g^{*0.5} + 0.397 j_f^{*0.5} = 0.603 - 0.00234 \left(\frac{L}{D} \right), \quad \text{for Kang's correlation} \quad (8)$$

where, L is the length of the riser (inclined section).

The predictions of the empirical correlations are compared with the experimental flooding data bank. Comparison of the present correlation with the database is displayed graphically in Fig. 5 and the percentage error is defined as:

$$error(\%) = \frac{1}{n} \times \sum \left| \frac{j_{ge}^{*0.5} - j_{gp}^{*0.5}}{j_{gp}^{*0.5}} \right| \times 100\%, \quad (9)$$

where, n = number of flooding data points

$j_{gp}^{*0.5}$ = predicted flooding gas dimensionless superficial velocity

$j_{ge}^{*0.5}$ = experimental flooding gas dimensionless superficial velocity

The present empirical correlation agrees well with the database within the prediction error, 8.7%. Ohnuki's correlation predicts Ohnuki's data within 9.4% and Kang's correlation predicts Kang's data within 2.9%. However, the Ohnuki's correlation and the Kang's correlation have the prediction error, 12.2% and 10.7%, respectively for the all database.

NO and Choi [12] developed a flooding correlation from their experimental studies of flooding in nearly horizontal pipes. It is interesting that the NO and Choi's flooding data is well predicted by the present empirical correlation as shown in Fig. 6.

3. Code and Model Description

3.1 Code Description

The assessment calculation for sample problems and CCFL experiments in the database are done using RELAP5/MOD3.2.2 γ computer code fixed for crossflow junction subscripts. Subscript errors were discovered by Won-Jai Lee (KAERI) in the vexplt subroutine for the crossflow junctions. These errors are known to affect the crossflow wall friction. Therefore, in a problem like CCFL, which has a cell with a crossflow junction, the patched code should be used. The correction in the vexplt subroutine was to change the kf and lf subscripts on rho_f and rho_g to k and l, respectively. The code is patched on SUNW SPARCstation 20 system operating under Solaris 2.6. The computer is a 32-bit workstation with 128MB of RAM memory and 167 MHz of clock speed.

In this study assessment of version 3.2.2 Gamma for CCFL in the horizontal-to-inclined pipes is done and the standard version is improved, as is the standard practice for developmental versions of RELAP5.

3.2 RELAP5 Nodalization

From the sample problems to test how RELAP5 code predicts the CCFL behavior in a pipe RELAP5 nodalizations have been developed for the simulation of the experiments in the database. The sample problems used in the present calculation is closely related to the test facilities used in many previous experiments for horizontal-to-inclined pipes. Most experiments were performed using air and water under atmospheric pressure. A general configuration of the test facility as shown in Fig. 1 is modelled to the RELAP5 nodalization in Fig. 7.

Water is injected into the test section (Pipe-100) from the right plenum (Branch-340) and air from the left plenum (Pipe-230). Flow boundary conditions of water and air are modelled as time dependent junctions, TDV-315 and TDV-215, respectively. Water is drained into the left plenum (Pipe-230) and time dependent junction, TDJ-250 controls the water inventory in the left plenum such that the flow rate to water outlet (TDV-260) is equal to the water flow rate from the test section. Air flows out to the right plenum and flows up into the upper plenum (Pipe-350). And then air is vented to time dependent volume, TDV-360 that is modelled as a pressure boundary.

The test section is modelled as a pipe component divided into horizontal volumes and inclined volumes. Flow area and the horizontal volume length of the test section are determined by D and L from the database. The inclination angle (θ) of the elbow is applied to the inclined volumes.

The present nodalization is similar to those used in reference [1] and [2]. However, some modelling change is applied to the present model. A “nearly zero injection flow” (10^{-300} of total water injection flow rate) is modelled as a time dependent junction (TDJ-316) between the horizontal volumes and the inclined volumes of the test section. Addition of flow boundary condition (TDJ-316) does not affect the amount of water inlet flow but removes the modelling deficiency explained in the next section.

3.3 Simulation Procedure

The RELAP5 calculations followed the experimental procedure of allowing the liquid flow to settle down into a steady state before increasing the gas injection. Water flow is ramped up from zero to a given flow rate corresponding to the dimensionless superficial liquid velocity of the simulated database. While the water flow is maintained constant, the air flow is increased slowly until the onset of flooding is observed.

The onset of horizontal flooding is brought out, in RELAP5, by the rapid and very large increase of interface friction, which happens as the flow regime changes from stratified to slug flow. And the transition from stratified to slug flow induces the oscillatory behavior of void fraction, mass flow rate, pressure, and etc. Figure 8 shows the behavior of liquid and gas mass flow rates during the simulation of a sample problem.

At the moment the liquid flow rate in the horizontal test section has limitation and shows the fluctuation, the flooding gas flow rate is roughly determined. And after some trial and error calculations for the fixed water and air flow rates, we can obtain more correct flooding points.

3.4 Pre-Test Calculations of the Present Input Model

A small modelling change made to the present nodalization is tested how RELAP5 predicts the gradient of the liquid level in the horizontal test section. In the reference experiments for the present database the liquid flow is a free falling, that is, the void fraction at the exit region of liquid flow is 1. However, in the test problem the void fraction at the water outlet is maintained as 0.63 to see if the accelerated water velocity in the inclined region is reduced in the horizontal region and the liquid level is increased to an exit liquid level.

The variations of liquid fractions $(1-\alpha)$ with and without a nodalization change are shown in Fig. 9. The profile of the liquid fraction with a nearly zero injection flow (TDJ-316) represents well the gradient of water level in the test section. The liquid level is highest near the elbow and the liquid film is very thin in the inclined volumes. However the nodalization without TDJ-316 predicts very low water level in the horizontal volumes and even lower level than the liquid fraction (0.37) of an exit boundary condition. Therefore, it is not surprising that the input model without additional time dependent junction (TDJ-316) calculates higher superficial gas velocity for the onset of flooding than the present model with TDJ-316.

The unreasonably low water level is also found in the predictions of RELAP5/MOD2 [2] and RELAP5/MOD3 [2] of which nodalizations have not such a nearly zero injection model as TDJ-316 in the present nodalization.

The effect of TDJ-316 on the prediction of liquid level can be explained by the unexpected condition in the calculation of volume-average velocity of RELAP5.

The liquid and vapor velocities in the volume cells are calculated by a method that averages the phasic mass flows over the volume cell inlet and outlet junctions. A cell volume is shown in Fig. 10, where each arrow into the volume cell represents the liquid mass flow from the inclined section and a nearly zero liquid mass flow, respectively. The arrow out of the volume cell represents the liquid mass flow through outlet junction and there is no change in mass flow through an inlet and outlet junctions.

The RELAP5/MOD3 volume-averaged velocity formula (Eq. 3.1-198 in Ref. [13]) has the form:

$$(v_f)_L = \frac{\sum_{j=1}^{Jin} (\mathbf{a}_f \mathbf{r}_f v_f)_j A_j \cdot \sum_{j=1}^{Jin} A_j + \sum_{j=1}^{Jout} (\mathbf{a}_f \mathbf{r}_f v_f)_j A_j \cdot \sum_{j=1}^{Jout} A_j}{A_L \sum_{j=1}^{Jin+Jout} (\mathbf{a}_f \mathbf{r}_f)_j A_j}, \quad (10)$$

where, A is the junction area, A_L is the volume cross-sectional area defined in Eq. (3.1-190) of Ref. [14], subscript, j is the junction index, Jin is the number of inlet junctions, and Jout is the number of outlet junctions.

Then the volume-averaged liquid velocity in the cell volume with and without a nearly zero injection flow, $(v_f)_{L1}$ and $(v_f)_{L0}$ can be derived, respectively as:

$$(v_f)_{L1} = \frac{[(\mathbf{a}_f \mathbf{r}_f v_f)_1 A_1^2 + (\mathbf{a}_f \mathbf{r}_f v_f)_2 A_2^2] + [(\mathbf{a}_f \mathbf{r}_f v_f)_1 A_1 A_3]}{A_L [(\mathbf{a}_f \mathbf{r}_f)_1 A_1 + (\mathbf{a}_f \mathbf{r}_f)_2 A_2] + [A_L (\mathbf{a}_f \mathbf{r}_f)_3 A_3]}, \quad \text{with TDJ-316} \quad (11)$$

$$(v_f)_{L0} = \frac{[(\mathbf{a}_f \mathbf{r}_f v_f)_1 A_1^2 + (\mathbf{a}_f \mathbf{r}_f v_f)_2 A_2^2]}{A_L [(\mathbf{a}_f \mathbf{r}_f)_1 A_1 + (\mathbf{a}_f \mathbf{r}_f)_2 A_2]}. \quad \text{without TDJ-316} \quad (12)$$

We can see that two terms, $[(\mathbf{a}_f \mathbf{r}_f v_f)_1 A_1 A_3]$ in the numerator and $[A_L (\mathbf{a}_f \mathbf{r}_f)_3 A_3]$ in the denominator are added to Eq. (12) for the nearly zero injection flow model (TDJ-316). Therefore, a nearly zero injection flow model is effective when the junction area (A_3) is nonzero. Then the velocity ratio, $(v_f)_{L1}/(v_f)_{L0}$ is investigated when the additional junction area (A_3) is increased infinitely to see the effect of a nearly zero injection flow model on the change of volume-average velocity.

$$\lim_{A_3 \rightarrow \infty} \frac{(v_f)_{L1}}{(v_f)_{L0}} = \lim_{A_3 \rightarrow \infty} \frac{[(\mathbf{a}_f \mathbf{r}_f v_f)_1 A_1 A_3]}{[A_L (\mathbf{a}_f \mathbf{r}_f)_3 A_3] (v_f)_{L0}} = \frac{\dot{m}_f}{\mathbf{r}_f A_L (v_f)_{L0}} \quad (13)$$

If we define the liquid fraction and the mass flow rate in the cell volume without a nearly zero injection flow as $(\mathbf{a}_f)_{L0}$ and $(\dot{m}_f)_{L0}$, respectively, the Eq. (13) can be expressed as:

$$\frac{\dot{m}_f}{\mathbf{r}_f A_L (v_f)_{L0}} = \frac{\dot{m}_f (\mathbf{a}_f)_{L0}}{(\dot{m}_f)_{L0}} = (\mathbf{a}_f)_{L0} < 1 \quad (14)$$

where, the mass flow rate at inlet and outlet of cell volume is conserved and the flow regime is horizontally stratified.

Knowing that Eq. (14) is smaller than 1 we can see that the velocity is reduced when the nearly zero injection flow model is used.

Figure 11 shows that RELAP5 calculation of the volume-average velocity is decreased as the area ratio of TDJ-316 to main test section (A_3/A_1) is increased. For the liquid fraction the trend is reversal because of the mass conservation in the cell volumes as shown in Fig. 12.

Therefore, the present input model with a nearly zero injection model simulates the liquid velocity, which is accelerated in the inclined region by gravitation and decreased in the horizontal region by wall friction. The reduced velocity in the horizontal cell volumes increases the liquid level because of the mass conservation and shows well the gradient of water level from the bend to the exit.

The present input model developed from the calculations of test problems is used to obtain the RELAP5 predictions of the onset of flooding in this study.

4. Code Calculations of the Database

4.1 Length-to-Diameter Ratio (L/D) Effect on RELAP5 Predictions

The experimental results with different L/Ds are simulated by RELAP5. For the same dimensionless liquid superficial velocity from experimental data critical gas superficial velocity is obtained by RELAP5. The range of L/D is from 3.0 to 58.0 as shown in Fig. 13. The relationship between L/Ds and critical gas flow rates required to initiate CCFL is also confirmed in RELAP5 calculations. Comparing the RELAP5 results with experimental data, we can see that RELAP5 predicts the flooding points closely but higher gas flow rates than those from real data where L/D is as low as that of the hot legs of typical PWR.

4.2 Inclination Angle (θ) of Elbow Effect on RELAP5 Predictions

RELAP5 calculations are compared with the flooding data points for different inclination angles. To avoid the L/D effects on CCFL experimental results with same L/Ds ($=25$) are simulated by RELAP5. The calculation results and experimental data are plotted in Fig. 14. The percentage error between RELAP5 results and data points is within 2%. In RELAP5 calculations the flooding points are always the same for the different inclination angles, because the CCFL in the inclined region is less restrictive than in the horizontal region.

5. Application of Empirical Flooding Correlation to RELAP5

An empirical flooding correlation developed from the present database is applied to the RELAP5 CCFL model. It is known that the interfacial drag model and CCFL curve given by user mainly characterize the flooding process. Therefore, the interfacial and the wall drags are reduced when flooding occurs at lower gas velocity than predicted by the CCFL curve in standard RELAP5.

It is shown that the present flooding correlation is successfully implemented to standard RELAP5 in Figs. 15 and 16 where, flooding limit of the empirical correlation is higher or lower than the predictions of standard RELAP5, respectively. For a given liquid flow rate gas flow rate is increased to reach the flooding curve, and then the calculation results of the modified RELAP5 lie well on the line given by the empirical correlation.

In Fig. 15 L/D is such a small value that the standard RELAP5 predicts the higher gas flow than the experimental data. In this case, the flooding criterion is satisfied before the interfacial and the wall drags initiate CCFL. When L/D is high as shown in Fig. 16, the onset of flooding occurs before the flooding limit by the correlation is applied in the RELAP5 calculation. From the debugging process of the modified RELAP5 we

found that CCFL is mainly influenced by the wall friction drag. If we reduce the wall friction and the interfacial drag coefficients in the horizontal test section for the modified version, the RELAP5 predictions lie well on the flooding line as shown in Fig. 16.

6. Conclusions

A total of 356 experimental data for the onset of flooding are compiled for the data bank and used for the assessment of RELAP5/MOD3.2.2 γ predictions of Counter-Current Flow Limitation (CCFL) in horizontal-to-inclined pipes simulating a PWR hot leg. From the present study the following conclusions can be made.

- 1) The dimensionless Wallis-type gas velocities and liquid velocities are identified with the geometrical conditions such as horizontal pipe diameter (D), length (L) and the inclination angle (θ) of the bend. Most data show the trend where the lower L/D, the higher the flooding curve. However the θ effect on CCFL was not found.
- 2) The RELAP5 calculations are compared with the experimental data where L/D is varied within the range of database. The L/D effect on CCFL is also confirmed in RELAP5 results, but higher gas flow rate is required to initiate the flooding compared with the experimental data if the L/D is as low as that of the hot legs of typical PWRs.
- 3) The best fitting correlation is developed for the prediction of flooding points. The regression of the existing data points are conducted to find the constant m for the slope of flooding curve and the gas intercept, c. The results of empirical correlations based on the present data bank are as follows:

$$j_g^{*0.5} + 0.614 j_f^{*0.5} = 0.635 - 0.00254 \left(\frac{L}{D} \right)$$

- 4) We found that a nearly zero junction flow for one of multiple junctions causes the unexpected results in the calculation of volume-average velocity of RELAP5. The present input model with a nearly zero injection model simulates the liquid velocity that is accelerated in the inclined region by gravitation and decreased in the horizontal region by wall friction.
- 5) An empirical flooding correlation developed from the present database is applied to the RELAP5 CCFL model. It is shown that the present flooding correlation is successfully implemented to standard RELAP5 for the both cases where, flooding limit of the empirical correlation is higher or lower than the predictions of standard RELAP5.

REFERENCES

- [1] M. J. Dillstone, "Analysis of the UPTF Separate Effects Test 11(Steam-Water Countercurrent Flow in the Broken Loop Hot Leg) Using RELAP5/MOD3," NUREG/IA-0071, June 1992.
- [2] F. Curca-Tivig, "Assessment of RELAP5/MOD3/V5m5 Against the UPTF Test No. 11 (Countercurrent Flow in PWR Hot Leg)," NUREG/IA-0116, May 1993.
- [3] Richard A. Riemke, "Countercurrent Flow Limitation Model for RELAP5/MOD3," Nuclear Technology, Vol. 93, pp. 166-173, Feb. 1991.
- [4] Sun Heo and Hee Cheon NO, "Improvement of The CCFL Models of the RELAP5/MOD3.2.2B Code in a Horizontal Pipe," Proc. 8th International Conference on Nuclear Engineering, Baltimore, USA, April 2-6, 2000.
- [5] A. Ohnuki, "Experimental Study of Counter-Current Two-Phase Flow in Horizontal Tube Connected to Inclined Riser", J. of Nuclear Science and Technology, 23[3], pp.219-232, March 1986.
- [6] P. T. Wan and V. S. Krishnan, "Air-Water Flooding in 90° Elbow with a Slightly Inclined Lower Leg," Proc. CN 7th Annual Conf., Toronto, June 1986.
- [7] H. Siddiqui, S. Banerjee, and K. H. Ardron, "Flooding in a Elbow Between a Vertical and a Horizontal or Near-Horizontal Pipe," Int. J. Multiphase Flow, Vol. 12, No. 4, pp. 531-541, 1986.
- [8] M. Kawaji, L. A. Thomson, and V. S. Krisnan, "Countercurrent Flooding in Vertical-to-Inclined Pipes," Experimental Heat Transfer, Vol. 4, pp. 95-110, 1991.
- [9] G. Geffraye, P. Bazin, P. Pichon, and A. Bengaouer, "CCFL in Hot Legs and Its Prediction with the CATHARE Code," Proc. 7th Int. Meeting on Nuclear Reactor Thermal Hydraulics, NURETH-7, Saratoga Springs, New York, Sept. 1995
- [10] S. Wongwises, "Two-Phase Countercurrent Flow in a Model of a Pressurized Water Reactor Hot Leg", Nuclear Engineering and Design, Vol. 166, pp. 121-133, 1996
- [11] S. K. Kang and Hee Cheon NO et al., "Air-Water Countercurrent Flow Limitation in a Horizontal Pipe Connected to an Inclined Riser," J. Korean Nuclear Society, Vol. 31, No. 6, pp. 548-560, Dec. 1999.
- [12] K. Y. Choi and Hee Cheon NO, "Experimental Studies of Flooding in Nearly Horizontal Pipes", Int. J. Multiphase Flow, Vol. 21, No. 3, pp. 419-436, 1995.
- [13] K. E. CARLSON, R. A. RIEMKE, S. Z. ROUHANI, R. W. SHUMWAY, and W. L. WEAVER, "RELAP5/MOD3 Code Manual," Vol. I: Code Structure, System Models, and Solution Methods, NUREG/CR-5535, EGG-2596, EG&G Idaho, Inc. (June 1995).

Table 1. Experimental Flooding Data for CCFL in Horizontal-to-Inclined Pipe

Ref.	Tube diameter range (m)	Tube length range (m)	Inclination angle of riser (q)	Number of data points
Ohnuki (1986)	0.026, 0.076	0.01 ~ 0.4	$40^\circ, 45^\circ$	146
Wan (1986)	0.051	2.958	90°	18
Siddiqui (1986)	0.038 ~ 0.047	1.82 ~ 2.36	90°	32
Kawaji (1991)	0.051	2.54	90°	7
UPTF (1993)	0.75	7.086	50°	7
MHYRESA (1995)	0.351	2.645	50°	9
Wongwises (1996)	0.064	0.557 ~ 1.408	$50^\circ \sim 90^\circ$	104
Kang (1999)	0.04, 0.08	0.7 ~ 3.388	35°	33

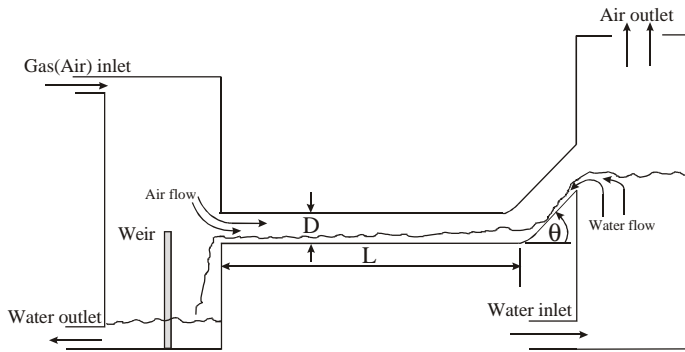


Fig. 1. General Configuration of the CCFL Test

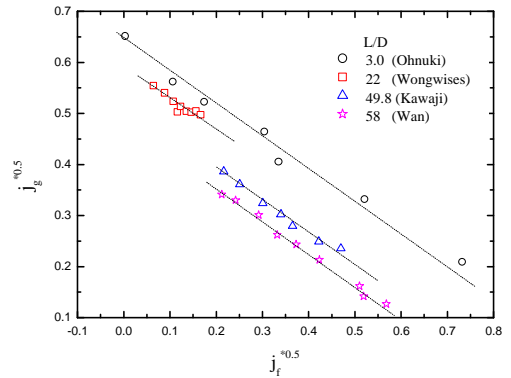


Fig. 3. Effect of Horizontal Pipe Length-to-Diameter Ratio on CCFL

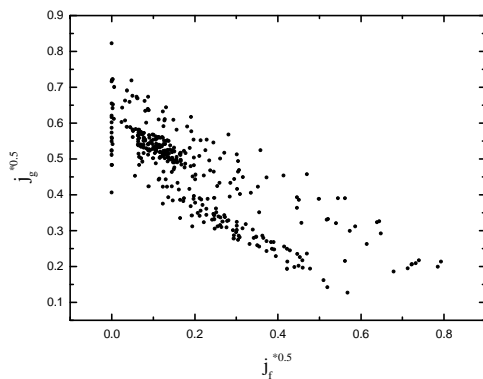


Fig. 2. Experimental Flooding Data Points

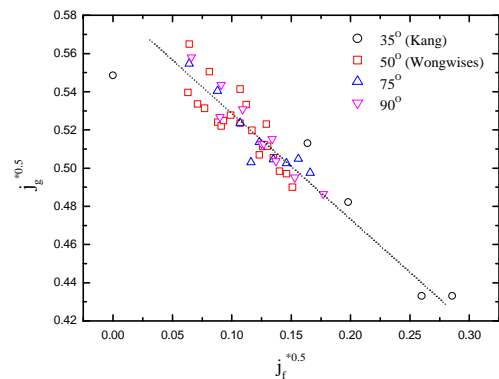


Fig. 4. Effect of Inclination Angle of Elbow on CCFL

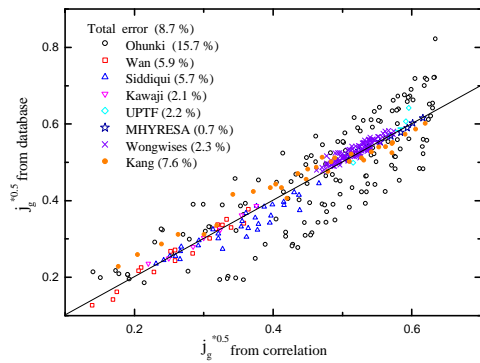


Fig. 5. Comparison between Eq. (6) and All Data in the Present Database

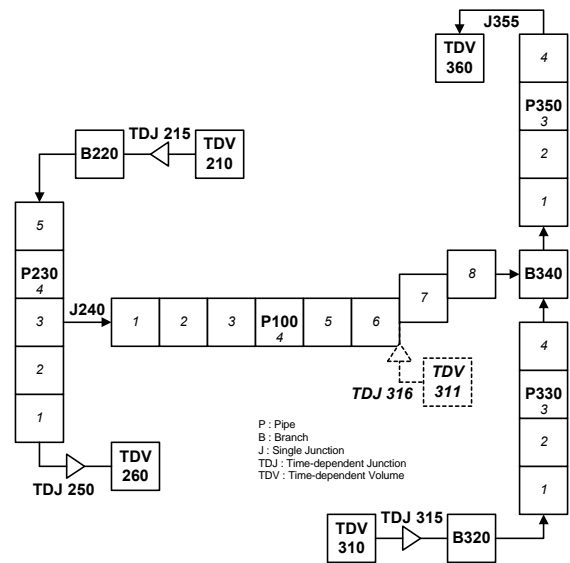


Fig. 7. RELAP5 Nodalization of CCFL Test in a Horizontal-to-inclined Pipe

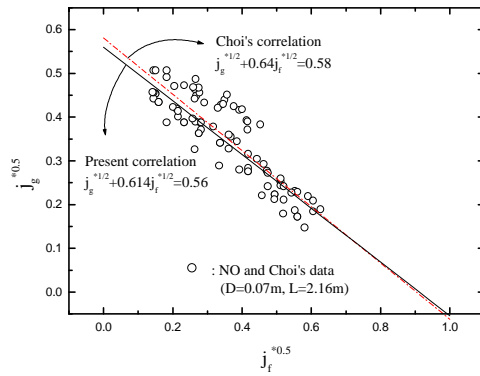


Fig. 6. Comparison between the Present Empirical Correlation and NO and Choi's Data

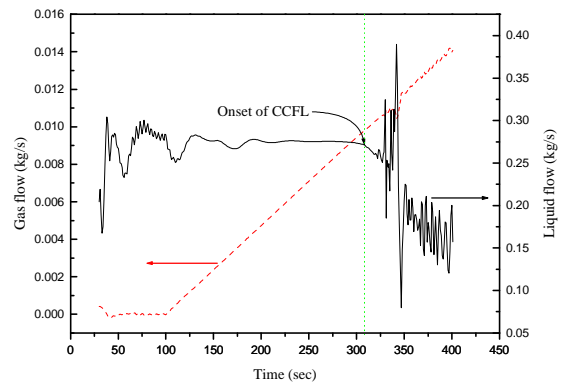


Fig. 8. Variation of Gas and Liquid Flow Rates at the Onset of CCFL

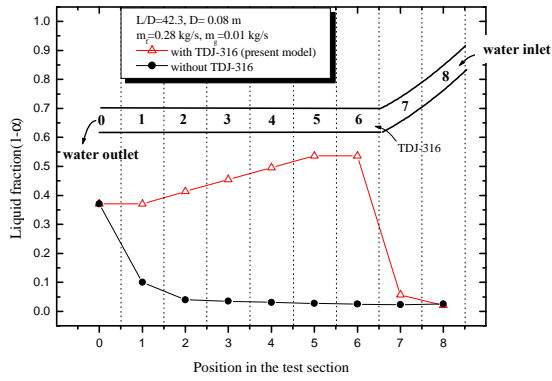


Fig. 9. Profile of the Liquid Fraction in the Air-water Countercurrent Flow

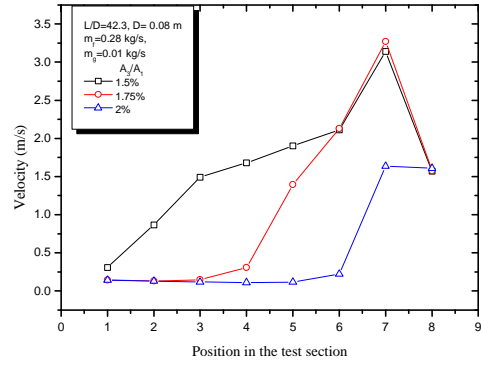


Fig. 11. Effect of TDJ-316 Area on the Volume-Average Velocity

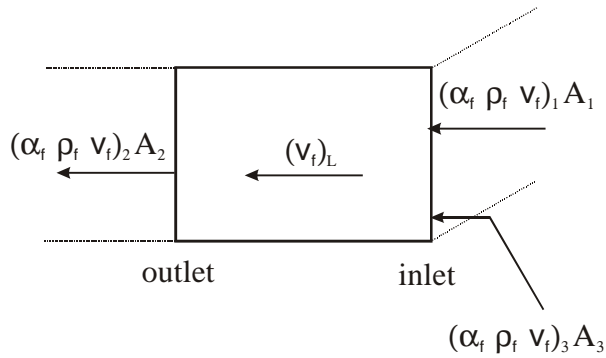


Fig. 10. Schematic of a Volume Cell with Inlet and Outlet Junction Mass Flows

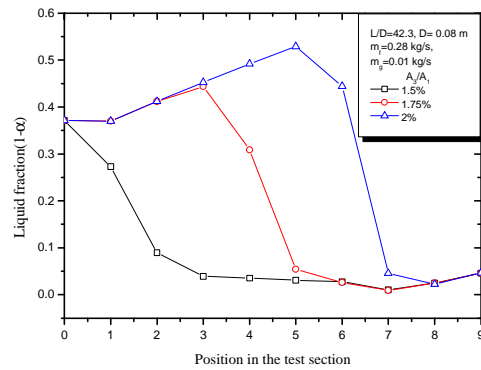


Fig. 12. Effect of TDJ-316 Area on the Liquid Fraction

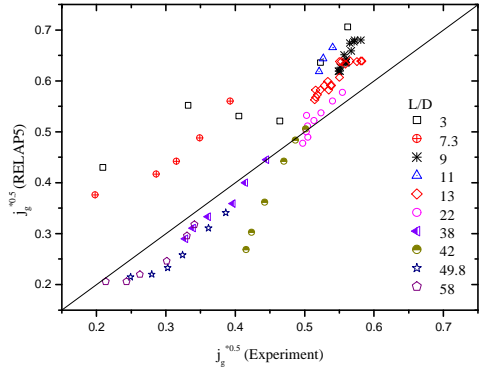


Fig. 13. Comparison of RELAP5 with Experimental Results of Various L/Ds

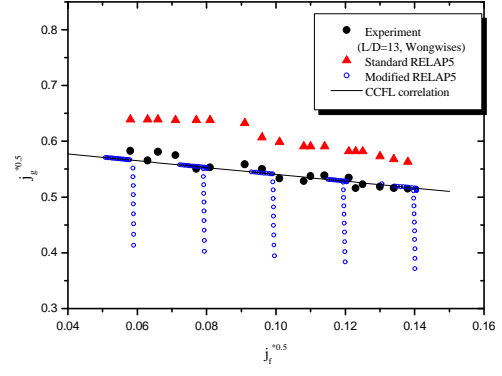


Fig. 15. Calculation of Over-predicted Data with the Modified RELAP5

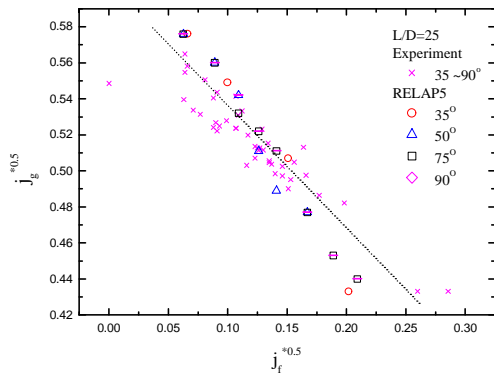


Fig. 14. Effect of Inclination Angle on RELAP5 Calculations

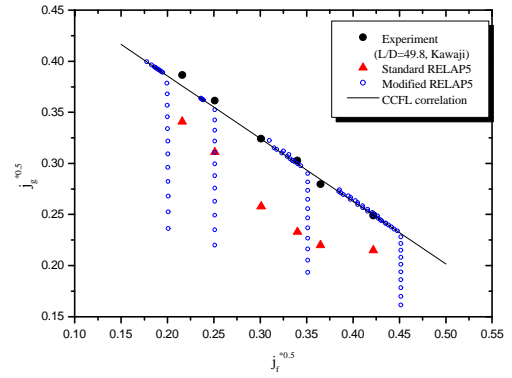


Fig. 16. Calculation of Under-predicted Data with the Modified RELAP5